Rheol Acta (2013) 52:467–483
DOI 10.1007/s00397-013-0704-8

ORIGINAL CONTRIBUTION

Aging, rejuvenation, and thixotropy in yielding magnetorheological fluids

Juan de Vicente · Claudio L. A. Berli

Received: 17 September 2012 / Revised: 27 March 2013 / Accepted: 4 April 2013 / Published online: 12 May 2013

Abstract The yielding behavior of dilute magnetorheological (MR) fluids has been investigated using creep–recovery tests. At very low stress levels, MR fluids behave in the linear viscoelastic regime as demonstrated by the fact that the instantaneous strain equals the instantaneous (elastic) recovery. In this region, gap-spanning field-induced structures support the stress levels applied. Upon increasing the stress value, the MR fluid evolves towards a nonlinear viscoelastic response. Here, the retarded elastic and viscous strain decrease, and the plastic contribution to the instantaneous strain grows probably due to the appearance of unattached field-induced structures. A larger stress value results in a viscoplastic solid behavior with negligible retarded and viscous strain and a fully plastic instantaneous strain. Finally, a plastic fluid behavior is found when the stress value is larger than the so-called yield stress. MR fluids exhibit an intermediate behavior between *non-thixotropic* (simple) and highly thixotropic model yield stress fluids.

Keywords Magnetorheology · Magnetorheological fluids · Creep · Recovery · Unsteady flow · Yielding · Phase diagram

Special issue devoted to novel trends in rheology.

J. de Vicente (✉)
Department of Applied Physics, Faculty of Sciences,
University of Granada, 18071 Granada, Spain
e-mail: jvicente@ugr.es

C. L. A. Berli
INTEC (UNL-CONICET),
Güemes 3450, 3000 Santa Fe, Argentina

Introduction

Magnetized magnetorheological (MR) fluids are known to exhibit nonequilibrium transitions from a fluid- to solid-like state, characterized by the sudden arrest of their dynamics. This phenomenology is ubiquitous to a wide variety of systems as already reported by Trappe et al. (2001). In this context, what makes MR fluids of especial interest is the fact that the jamming state of the constituent particles can be externally tuned by the application of magnetic fields. In other words, MR fluids can be considered smart attractive colloids as their interparticle (magnetic) attraction can be tuned externally.

In general, a colloidal system can be jammed by increasing the volume fraction of the constituents, increasing the interparticle attractions, or decreasing the stress. In this work, we will focus our attention in MR fluids that are jammed by increasing the magnetostatic interactions between the constituent particles for a constant volume fraction. Also, generally speaking, jammed solids have been reported to be refluidized by thermalization or by an applied stress, and consequently, a unified description has been proposed in terms of a jamming phase diagram for attractive colloidal particles that aimed to give a unifying link between the glass transition, gelation, and aggregation (Trappe et al. 2001). In this work, we are interested in unjamming the MR fluids under the application of shear stresses. Accordingly, we will be able to induce a solid- to fluidlike transition in MR fluids that are initially jammed at a given magnetic field strength and particle volume fraction, by simply applying a shear stress.

In rheological terms, jammed solids are typically identified by the appearance of a low-frequency plateau in the elastic modulus, a viscosity divergence, and eventually the

onset of a yield stress (the minimum stress value for the material to flow) under the conditions of experimentation. In spite of this apparently simple definition, the determination and also the existence of a true yield stress is still controversial (Moller et al. 2006).

Probably the most suitable technique to measure a yield stress is the so-called vane method (Barnes and Nguyen 2001). Unfortunately, the necessity of application of a magnetic field precludes the use of this technique. However, in spite of its difficulty, there are many different approaches to interrogate the yield stress in a MR fluid that are also employed in other pasty materials (see for instance Christopoulou et al. 2009; Laurati et al. 2011). In most cases, the yielding behavior has been ascertained by the application of shear stress or strain rate ramps. However, more reliable techniques have been employed in the literature, for example, using stress/strain amplitude sweeps (de Vicente et al. 2002, 2011). Among them, we would like to emphasize the use of creep tests. In a creep test, a constant shear stress is applied for a time interval, while the strain is recorded. These are very delicate methods, especially when accompanied by a recovery stage and, at large stresses, where tool inertia might prohibit instantaneous halt. Consequently, the literature on this is very scarce. Pioneering works that described the use of creep tests to investigate the yielding behavior of MR fluids are briefly summarized now. In 1994, Otsubo and Edamura (1994) reported creep data on electrorheological (ER) fluids. They showed that contrary to the expectation at that time, electrified ER fluids did not behave as pure elastic solids at low stresses but, instead, exhibited a retarded elastic and viscous flow. Interestingly, the recovery behavior was found to be purely plastic, for intermediate and large stresses, in disagreement with classical single-chain model predictions. In the ER fluids investigated, the yield stress value determined by creep tests was found to be smaller than the plateau stress in the flow curves. Li and coworkers (2002) investigated the effect of magnetic field strength and temperature on the creep behavior of MR fluids (below the yield value). Their results indicated that MR fluids behaved as linear viscoelastic bodies at very small stresses, with increasing constant stresses, nonlinear viscoelastic, viscoplastic, or purely plastic properties dominated. See et al. (2004) also reported creep tests on commercial MR fluids in the preyield regime. They demonstrated that shear compliance data collapsed at low stresses, well within the linear viscoelastic region. The elastic compliance was best fitted by a power law relationship $\propto H^{-4.4}$ in discrepancy with the simple dipole–dipole interaction model that predicts a scaling with H^{-2}. This finding was argued to reflect the fact that as the magnetic flux density is increased, the nature of structures themselves undergoes a change. In 2006, Chotpattananont et al. (2006) investigated the creep response of poly(3-thiopheneacetic acid) ER fluids. They demonstrated that similarly to MR fluids, the suspensions exhibited an evolution with an increase of applied stress from a linear viscoelastic response at low stresses to a nonlinear viscoelastic response, followed by a viscoplastic solid, and finally a transition from plastic solid to plastic liquid at the yield stress.

Creep–recovery tests have also been employed in the examination of the yielding behavior of other pasty materials. For example, creep–recovery measurements by Petekidis et al. (2003, 2004) demonstrated that hard-sphere (repulsive) colloidal glasses tolerate large strains, up to at least 15 %, before yielding irreversibly. A non-negligible recovery is found even in samples which have flowed significantly during stressing. Such a recovery is attributed to cage elasticity. The creep–recovery behavior of attractive colloidal glasses was investigated by Pham et al. (2008). In contrast to what occurred for hard-sphere colloidal glasses, the recovered strain exhibits a peak with stress, and a finite recovered strain is measured even well above the yield stress. More recently, a similar peak was also found when plotting the maximum recovered strain versus stress values in the case of colloidal gels by Laurati et al. (2011).

In this work, we are interested in a better understanding of the yielding behavior of MR fluids under the presence of uniaxial DC external magnetic fields. To do so, we carry out an extensive rheological study that involves steady and unsteady (shear) flows. Also, for a comparative purpose, model yield stress fluids are formulated ad hoc having similar yield stress values but exhibiting a very different thixotropic behavior. On the one hand, polyacrylic acid polymers are employed as model microgel dispersions that are essentially *non-thixotropic*. On the other hand, we use bentonite clay suspensions that are well-known to form very thixotropic yield stress fluids. Finally, time-dependent changes in viscosity are explained in terms of the thixotropic structural model developed by Quemada (2008).

Theory

Time-dependent rheological phenomena appearing in gels, pastes, and colloidal glasses can be rationalized in terms of structural viscosity models (Quemada 1998, 2008; Derec et al. 2001; Coussot et al. 2002; Derec et al. 2003; Craciun et al. 2003; Moller et al. 2009b). This kind of modeling grounds is on three basic concepts: (a) a structural variable S characterizing the structure, (b) a rate equation of S that accounts for the forces perturbing the microstructure (viscous forces from the gradient velocity field) and those restoring the equilibrium state (Brownian motion and interparticle forces), and (c) a given form of the viscosity–structure relation, $\eta(S)$.

In the model proposed by Quemada (1998), the structural state of dispersion is regarded as a mixture of individual particles and clusters of them (structural units) suspended in a fluid. The structural variable S is defined as the number fraction of particles contained in the structural units. The time dependence of S results from the balance between buildup and breakdown of structural units, which is governed by the following relaxation kinetics:

$$dS/dt = \left(t_{\mathrm{Br}}^{-1} + t_{\mathrm{in}}^{-1}\right)(1 - S) - t_{\mathrm{hy}}^{-1}\, S \tag{1}$$

where t_{Br}, t_{in}, and t_{hy} are the characteristic relaxation times associated to Brownian, pair interaction, and hydrodynamic forces, respectively. According to the definition given above, S enters the effective volume fraction of the disperse phase, $\phi_{\mathrm{eff}} = \phi\,(1 + CS)$, where ϕ is the true particle volume fraction, and C is a compactness factor. It is observed that $\phi_{\mathrm{eff}} \geq \phi$, because the effective volume fraction includes the volume occupied by the particles plus the volume of solvent immobilized hydrodynamically in the structural units. Finally, the shear viscosity is obtained by introducing $\phi_{\mathrm{eff}}(S)$ into the following equation:

$$\frac{\eta}{\eta_{\mathrm{F}}} = \left(1 - \frac{\phi_{\mathrm{eff}}}{\phi_{\mathrm{m}}}\right)^{-2} \tag{2}$$

which generalizes a relationship between viscosity and volume fraction for concentrated colloidal dispersions (Quemada 1977; Brady 1993; Heyes and Sigurgeirsson 2004). In Eq. 2, η_{F} is the suspending fluid viscosity, and ϕ_m is the maximum packing fraction.

More recently, this modeling was extended to discuss time-dependent phenomena like thixotropy, aging, and rejuvenation by inserting a time-dependent solution of the kinetic equation $S(t)$ in the viscosity relation $\eta(S)$ under an unsteady shear (Quemada 2008). The details of the resulting "nonlinear structural" (NLS) model are not simple to be summarized, and the reader is referred to the original paper for further information. Here, we briefly describe the main rheological features that are of interest in the present work.

In the theoretical context of hard-sphere suspensions, if ϕ_{eff} is relatively high, the motion of structural units becomes strongly constrained due to the presence of neighbors, and the systems undergo a glassy transition when ϕ_{eff} reaches $\phi_g = 0.58$. If ϕ_{eff} further increases, the vibrational motion of particles vanishes at $\phi_{\mathrm{m}} \approx \phi_{\mathrm{RCP}} = 0.637$, the concentration of random close packing. Taking into account that ϕ_{eff} evolves in time, the model considers that the material is in a *fluid* phase for $\phi_{\mathrm{eff}} < \phi_g$, and in a *paste* phase for $\phi_g \leq \phi_{\mathrm{eff}} \leq \phi_{\mathrm{RCP}}$. Furthermore, there exists a critical volume fraction ϕ_{c2} that divides the paste domain into two: if the true volume fraction is $\phi < \phi_{c2}$, $\phi_{\mathrm{eff}}\,(t \to \infty)$ remains lower than ϕ_m, the steady state viscosity is finite, and the system is called a *soft* paste. In contrast, if $\phi \geq \phi_{c2}$, $\phi_{\mathrm{eff}}\,(t \to \infty)$ reaches ϕ_m, the viscosity *diverges*, and the material is called a *hard* paste. Therefore, for the system at rest, the NLS model predicts a *bifurcation* of the rheological behavior.

Accordingly, when the system is subjected to a constant shear stress τ, imposed after a destructuring step (preshear), the viscosity evolves as shown in Fig. 1a. For $\tau \leq \tau_Y$, the buildup of structure overcomes shear destructuring, and the viscosity tends to infinity. For $\tau > \tau_Y$, the structuring–destructuring processes attain a dynamical equilibrium, and steady viscosity plateaux are expected. As a consequence, a bifurcation is observed when τ reaches a critical value τ_Y, which only exists for $\phi_{c2} \leq \phi \leq \phi_m$. For particle concentrations lower than ϕ_{c2}, there is no sufficient structure to produce a bifurcation, even at zero shear stress.

As indicated in Fig. 1a, the region of $\tau \leq \tau_Y$ is associated to the phenomenon of *aging*, which is characterized

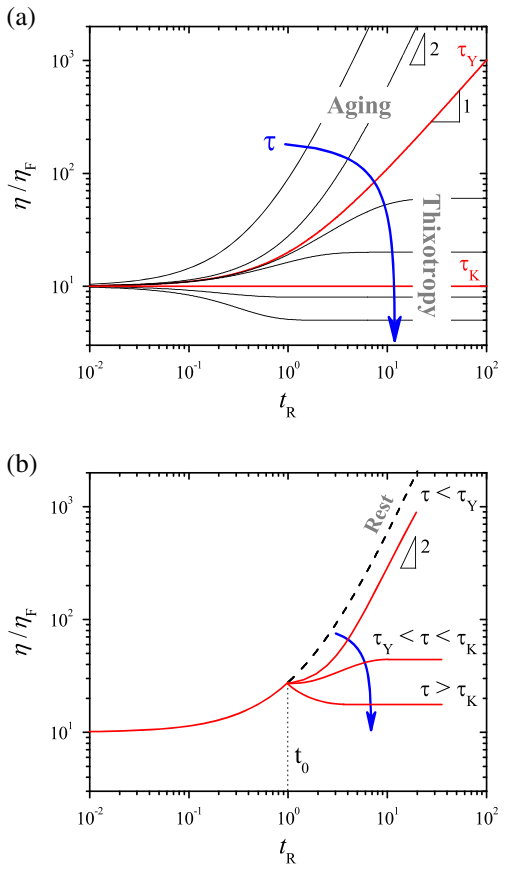

Fig. 1 **a** Relative viscosity as a function of dimensionless time, $t_R = t/(t_{Br} + t_{in})$, for *pastes* under constant shear stress, as predicted by Quemada's model (Quemada 2008). Arbitrary values of model parameters were used in calculations to qualitatively illustrate the viscosity bifurcation phenomena. τ increases from *top* to *bottom*. **b** Relative viscosity as a function of dimensionless time for pastes under constant shear stress after aging at rest

by the absence of equilibrium (no steady state viscosity is attained), and the slowing down of the evolution with a characteristic time that is proportional to the *age* of the system. Instead, the region of $\tau > \tau_Y$ corresponds the phenomenon classically known as *thixotropy*, where a steady state viscosity value is reached after a characteristic time that depends on Brownian motion and interparticle forces. Also in this region, the model predicts the existence of a stress τ_K where the system remains unaltered in its initial state ($S = S_{init}$). This stress value cannot be considered as an intrinsic characteristic of the material, since its value depends on the initial structure. When the stress $\tau_Y < \tau < \tau_K$, increasing the viscosity from its initial value corresponds to restructuring ($dS/dt > 0$). In contrast, when $\tau > \tau_K$, decreasing the viscosity from its initial value corresponds to destructuring ($dS/dt < 0$).

If the constant shear stress follows a rest period, depending on its length, the initial structure changes. In general, the longer the rest time is, the larger is the structural variable S. Interestingly, in the NLS model, the stress bifurcation is intrinsically independent of initial conditions, in contrast to predictions of Coussot and coworkers (2002, 2006). It is also possible that, depending on the material under study, the sample significantly ages during the rest period. Actually, this will be the case of highly thixotropic, bentonite clay suspensions studied in this work. If $\phi \geq \phi_{c2}$, the material ages with a viscosity that grows as t^2, and there are three possibilities depending on the level of the stress applied (see Fig. 1b): (a) for very low stresses ($\tau < \tau_Y$), structuring continues with a viscosity that diverges as t^2; (b) for intermediate stresses ($\tau_Y < \tau < \tau_K$), structuring increases but reaches a finite value; and finally, (c) for very large stresses ($\tau > \tau_K$), a maximum is initially reached, and then the viscosity decreases to reach a steady value.

The steady state ($t \to \infty$) response of systems with $\phi_{c2} \leq \phi \leq \phi_m$ subjected to $\tau > \tau_Y$ is that of fluids with a yield stress τ_Y. In this case, the model predicts the following steady shear viscosity:

$$\eta(\tau) = \eta_\infty \left(\frac{\tau + \tau_C}{\tau - \tau_Y} \right)^2, \tag{3}$$

where η_∞ is the high shear viscosity, and τ_C is a critical shear stress. Of course, if $\tau \leq \tau_Y$, $\eta \to \infty$ and $\dot{\gamma} = 0$. This nonlinear plastic behavior represents quite well several experimental results (see, for example, Berli and Quemada 2000).

Finally, we mention the structural model proposed by Coussot et al. (2002), which also involves a structural variable that evolves following a linear kinetics, and is empirically related to the shear viscosity η. Despite this model lacks of a detailed description of the micro- or mesostructure, it is able to capture some features of the macroscopic response, notably the viscosity bifurcation, and thus also helps to rationalize experimental results (Moller et al. 2006, 2009a).

Materials and methods

Conventional MR fluids were formulated by dispersing carbonyl iron microparticles (HQ grade, BASF) in silicone oils (20 ± 3 and 487 ± 2 mPa·s, Sigma-Aldrich) without additives. The particle volume fraction was fixed at 5 vol%. Accordingly, the MR fluid is expected to operate in the strong link concentration regime where the storage modulus increases with increasing the concentration, while the yield strain decreases with increasing the particle content (Segovia-Gutiérrez et al. 2012). This prevents complications that appear for larger concentrations where a two-step yielding process has been recently described (Segovia-Gutiérrez et al. 2012). Model yield stress fluids employed in the second part of this manuscript were prepared from aqueous dispersion of polyacrylic acid polymers (Sigma-Aldrich) and bentonite clay (Sigma-Aldrich). On the one hand, microgel suspensions were prepared from the neutralization of polyacrylic acid solutions at a concentration of 0.5 wt%. On the other hand, the clay volume fraction was fixed at 10 wt%.

Rheology experiments were conducted in a stress-controlled MCR 501 magnetorheometer (Anton Paar) to explore the yielding behavior of MR fluids in the presence of magnetic fields ranging from 52 to 259 kA/m. A plate–plate geometry (diameter 20 mm) was used. The temperature of the sample was stabilized at 25 °C using a circulating fluid bath. According to the manufacturer, the technical specifications of the rheometer were as follows: the minimum and maximum torques were 0.1 μNm and 230 mNm, respectively. On the other hand, the minimum and maximum speeds (in CSS mode) were 10^{-7} and 3,000 min^{-1}, respectively. It is worth to stress here that all experimental data reported in this study, although noisy in some cases, are well inside the specifications of the rheometer. Finally, it is worth to remark that slip was not observed during the experiments, and therefore, the rheometer tools were not surface treated (Segovia-Gutiérrez et al. 2012).

First, steady shear flow tests were carried out as described in Segovia-Gutiérrez et al. (2012). Briefly, the experimental procedure is summarized as follows: (a) initially, the sample was preconditioned at a constant shear rate 200 s^{-1} for 30 s; (b) next, the suspension was left to equilibrate for 1 min in the presence of a magnetic field; and (c) finally, the shear stress was logarithmically increased from 0.1 Pa at a rate of ten points per decade. Experiments were repeated at least three times with fresh new samples. The yield stress in the MR fluids is typically determined

using two different approaches. The first one consists in the determination of the so-called static yield stress as the stress corresponding to the onset of flow in double logarithmic representations of stress versus shear rate. A second method to determine the yield stress is to fit the Bingham plastic equation to a rheogram (shear stress versus shear rate) in lin–lin representation. The latter procedure results in the so-called Bingham yield stress that depends on the range of shear rates considered. Even though there are other more appropriate methods to measure the yield stress, these two approaches are frequently used in the MR literature (Volkova et al. 1999; de Vicente et al. 2002). For the purpose of this study, we are interested in the static yield stress.

Step stress and recovery tests were also performed under shear. The experimental protocol used is summarized in Fig. 2 as follows: (a) a preshear was first applied to eliminate shear history effects during 30 s (shear rate 100 s^{-1}); (b) an equilibration step followed at rest in a quiescent state (stress equal to zero), again during 30 s; (c) the magnetic field was suddenly applied during 120 s to promote the field-induced structuration; and (d) finally, step stress and recovery tests followed still in the presence of the magnetic field. In a typical essay, a constant shear stress τ_0 was applied for a time of 300 s, while the resulting strain was measured. The stress was then removed, and the recovered strain was measured for another 300 s. In all cases investigated, the strain was reset to zero at the beginning of the creep test.

Steady shear rheology of MR fluids

Figure 3a shows steady shear flow curves for 5 vol% MR suspension in 20 mPa·s silicone oil under different magnetic fields. In the absence of magnetic fields, the sample behaves as a Newtonian fluid (results not shown). However, in the presence of magnetic fields, the stress increases over the entire range of shear rates. In this figure, it is clearly shown that the MR fluid exhibits a yield stress, as a result of strong magnetic interactions among particles. The full lines in Fig. 3a represent Eq. 3, which is the steady state prediction of the structural viscosity model for effective volume fractions entering the paste phase, therefore leading to a plastic-like behavior. Yield stress values in Fig. 3a are clearly defined and hence model-independent. It is worth

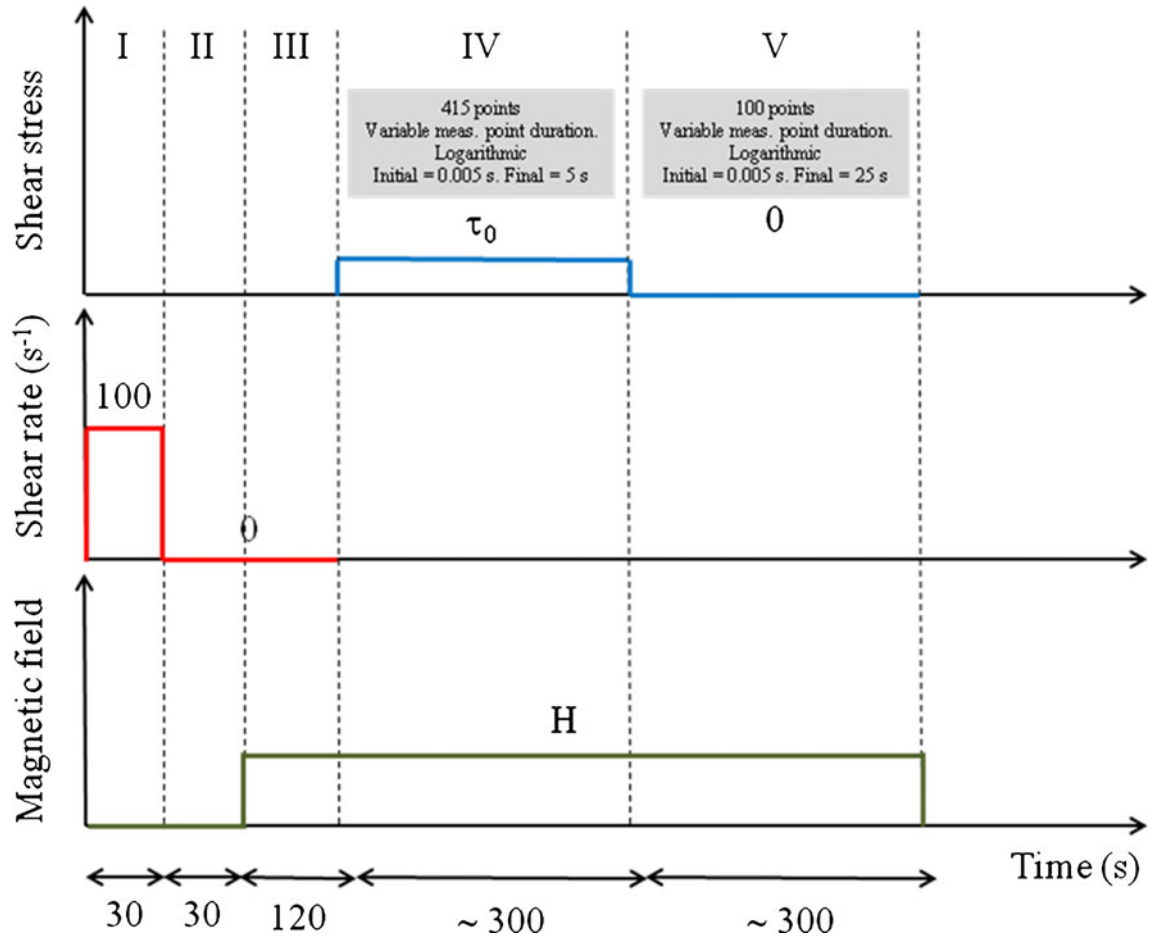

Fig. 2 Schematic of the protocol used for the creep–recovery investigations. Not to scale

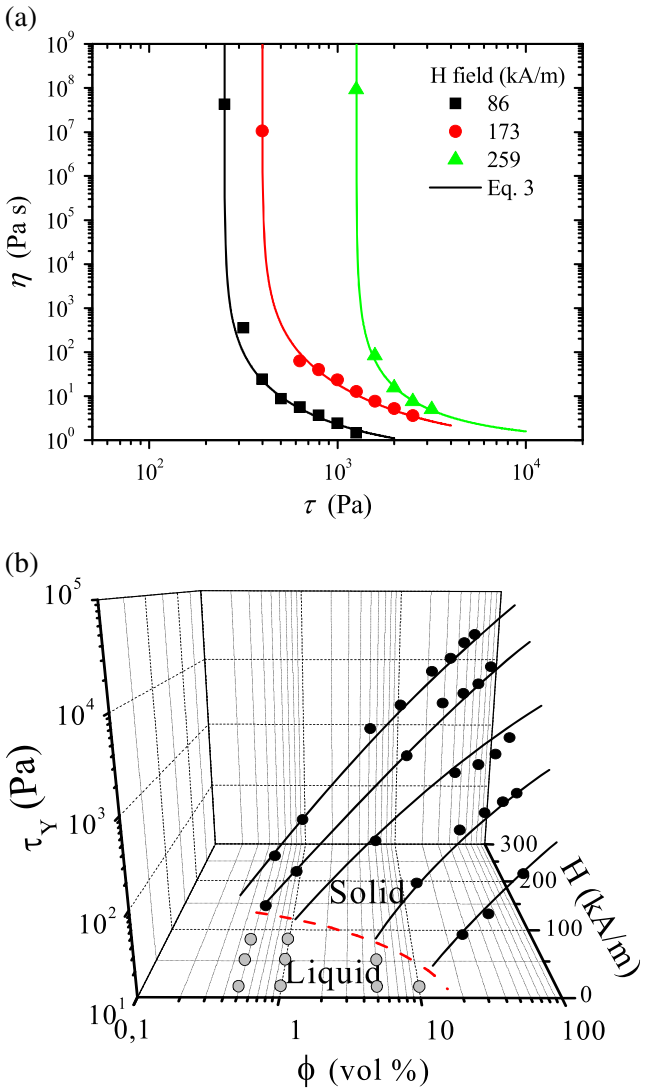

Fig. 3 **a** Steady shear flow curves for 5 vol% MR suspension in 20 mPa·s silicone oil in different magnetic fields. *Symbols* are experimental data. *Full lines* represent the structural viscosity model (Eq. 3; see text for details). **b** Three-dimensional jamming phase diagram for carbonyl iron-based MR fluids defined by the apparent yield stress (*black symbols*) as a function of both magnetic field strength and particle concentration (*lines* are used to guide the eyes). *Gray symbols* correspond to liquid states

noting, however, that the $\eta(\tau)$ trend of these suspensions cannot be described by the linear Bingham model.

On the other hand, if the applied magnetic field is relatively low (below ≈10 kA/m), the effective volume fraction (particle aggregates) is not sufficiently high, and the system is fluidlike for the whole range of shear rates and time scales explored in the experiments (Segovia-Gutiérrez et al. 2013). Eventually, a low-shear Newtonian plateau could be attained within an appropriate experimental window, as it was discussed in a recent work (Berli and de Vicente 2012).

In collecting data from a series of experiments analogous to that reported in Fig. 3a, at different particle volume fractions, we were able to build a three-dimensional jamming phase diagram for carbonyl iron-based MR fluids, which is shown in Fig. 3b. This figure closely resembles that reported in Fig. 3, in Trappe et al. (2001), and suggests the applicability of the jamming transition in describing aggregated MR fluids for a fixed time scale. Projecting the data plotted in Fig. 3b (yield stress) over the ϕ-H-plane defines a phase boundary that visibly differentiates fluid- and solid-like states. The transition can be reached either by increasing ϕ at a constant attractive interaction energy or by increasing the strength of particle–particle interactions at a given value of ϕ. The second possibility is normally used in the practice with MR fluids, where the attractive interaction is controlled by means of the external magnetic field H. A similar phase diagram can be obtained from a series of magnetosweep tests at fixed particle concentrations (Segovia-Gutiérrez et al. 2012). The resulting phase diagrams are in qualitative good agreement with the one obtained from steady shear flow tests described above. However, now, the critical field is found to be less sensitive on the particle concentration and one order of magnitude smaller, probably due to the different time scales employed in both steady and dynamic oscillatory shear tests. These results are not shown here for brevity.

The phase diagram also illustrates that the higher the attractive interaction is, the lower is the critical concentration ϕ_c required to reach a solid-like state in agreement with Trappe et al. (2001). This remarkable feature can be accounted for as a diminution of ϕ_c with the strength of the interaction. In fact, high values of ϕ are required to reach the solid-like threshold when the magnetic attraction is weak, since flocs continuously reorganize to form relatively small, compact clusters that are not enough to crowd the system. At the other extreme, when the interaction is strong, particle aggregation yields large, loosely packed clusters that easily jam to form an elastic solid, even at low values of ϕ. The critical volume fraction ϕ_c defined by Trappe et al. (2001) corresponds to ϕ_{c2} in the structural model of Quemada (2008), i.e., the minimum concentration required to attain a divergence of the shear viscosity, for a given interaction energy.

One may conclude that Fig. 3b resumes the role of particle concentration, interaction energy, and shear stress in the solid-like transition of MR fluids. To our knowledge, the phase behavior of MR fluids had not been discussed in this scenario before. This is important from the fundamental point of view (one observes that MR fluids present a universal phenomenology sheared with colloidal suspensions, emulsions, and microgels) (Trappe et al. 2001; Christopoulou et al. 2009; Laurati et al. 2011) and also has consequences in practice (for example, it is evident that the

critical H depends on ϕ and vice versa, which is relevant to formulate MR fluids for a given purpose).

Yielding behavior of MR fluids from step stress tests

As a way of example, Fig. 4a shows typical creep curves at shear stresses of 50, 150, 250, 400, 600, 1,000, 1,500, and 1,800 Pa, measured at a magnetic field strength of 173 kA/m. From Fig. 3a, the yield stress at 173 kA/m is estimated as c.a. 400 Pa under a steady flow. Hence, under the classical Bingham plastic point of view, for stresses below 400 Pa, the MR fluid is expected to behave as a elastic solid. However, a close observation of Fig. 4a reveals three regions at the lowest stress values investigated: instantaneous, retardation, and constant rate that are in contradiction with an elastic solid behavior. When the stress is first applied, there is a sudden, almost instantaneous increase of strain in less than 1 s. This is followed by a slight increase over the next 300 s. For the largest stresses investigated, a steady state regime is reached where the sample flows. The fact that the strain linearly increases with time at the longest times suggests the development of a viscous flow that will not be recovered upon cessation of the stress. It is of outstanding interest the observed stepwise increase in strain for a stress of 1,000 Pa (see inset in Fig. 4b) that has been associated in the past to unstable flows and/or aggregation fragmentation processes. Similar observations have been reported for MR fluids by See et al. (2004) (see Fig. 3b in their paper) and in the case of ER fluids by Otsubo and Edamura (1994) (see Fig. 5 in their paper).

Typical recovery curves are also shown in Fig. 4a. Interestingly, the deformation is very slightly recovered when removing the stress, in contrast to linear viscoelastic theory where the instantaneous elastic strain on the application and removal of stress must be the same. The instantaneously recovered strain defined as the strain which the sample recovers instantaneously after the removal of the stress is very small. Also, the total recovered strain, defined as the difference between the strain at the end of the recovery period and the maximum strain attained at the end of the creep period, is essentially the same as the instantaneously recovered strain. Since the strain is not completely recovered after the removal of the stress, the MR fluid is behaving as a purely plastic material, and the minimum (critical) stress associated to the onset of plasticity corresponds to the yield value. Since wall slip was not observed in the experiments, the plastic response is a consequence of bulk properties in the MR fluids. Interestingly, the instantaneous initial deformation without elastic recovery cannot be explained by the single-width chain model. In contrast, the deformation and rearrangement of particles in thick columnar structures have been argued to be responsible for

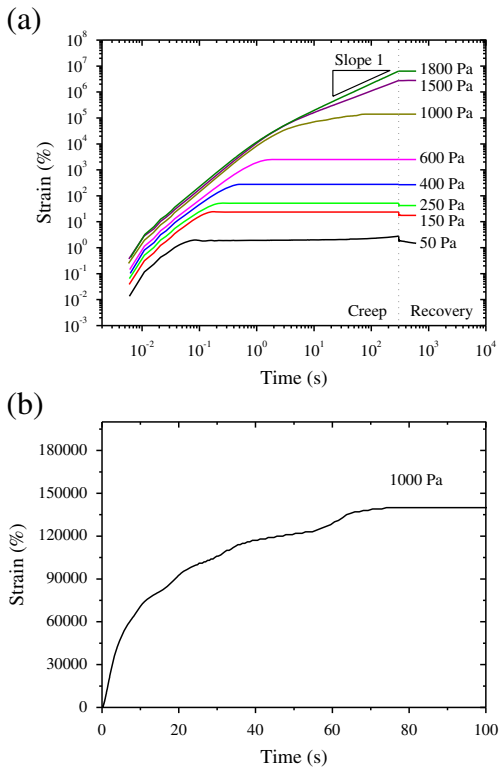

Fig. 4 (**a**) Time dependence of the shear strain achieved during a step stress (creep) and recovery experiment at 5 vol% MR fluid for several stresses as indicated in the figure. The magnetic field strength is 173 kA/m (**b**) detail for 1000 Pa

the purely plastic responses of MR fluids in the literature (Otsubo and Edamura 1994; Li et al. 2002; See et al. 2004).

More quantitative information on the yielding phenomena of MR fluids is obtained when plotting the instantaneous, or the total recovered strain, as a function of the applied stress (Fig. 5) as it may give a measure of energy storage. As commented above, both magnitudes give extremely similar values. Results shown in Fig. 5a reveal that the recovered (elastic) strain is essentially proportional to the stress at low stress values. In fact, from this proportionality constant, at very low stress values, the storage modulus can be estimated (Petekidis et al. 2003). The instantaneous strain decreases with increasing the magnetic field strength. This was expected as the elastic modulus is known to increase with the magnetic field strength. Similar results were obtained by Li et al. (2002) and See et al. (2004).

For large stresses, the total recovered strain reaches a maximum and then decreases. The maximum and, therefore, the onset of nonlinearity are achieved at the same strain value (10 %) independently of the magnetic field employed. This finding is in good agreement with the crossover yield strain γ_C (i.e., the strain corresponding to $G' = G''$) reported by Segovia-Gutiérrez et al. (2012) and resembles the recovery observed for attractive colloidal glasses by Pham et al.

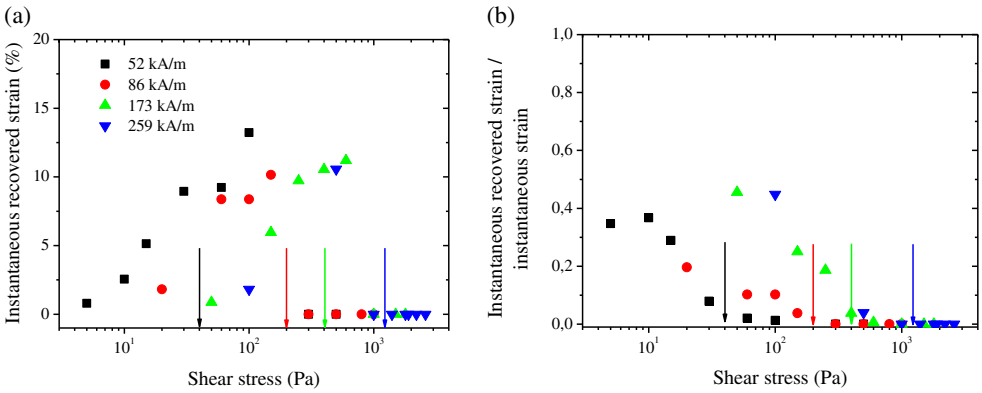

Fig. 5 Stress dependence of (**a**) the instantaneously recovered strain and (**b**) the ratio between the instantaneously recovered strain and the instantaneous strain. *Vertical arrows* correspond to the static yield stress as obtained from the extrapolation to zero shear rate of the flow curves in log–log representation (see Fig. 3b)

(2008) and colloidal gels by Laurati et al. (2011). This finding further implies that the energy required for particle arrangement is directly related to the strain level. The stress value corresponding to the transition from elastic deformation at small stresses to Newtonian flow at large stress (i.e., at the maximum) is an indicator of the yield stress of the material. In fact, Fig. 5b demonstrates that there is a reasonably good correlation between the stress values where the ratio between the instantaneously recovered strain and the instantaneous strain becomes zero and the yield stress obtained from steady shear flow curves (arrows in Fig. 5b). The recovery (elasticity) decreases with increasing the stress and reaches zero at the yield stress value. This finding is in good agreement with experiments on commercial MR fluids reported by Li et al. (2002). Also, with increasing the field strength at a fixed stress value, the viscoplastic response diminishes, and more elastic behavior ensues.

The creep and recovery behavior of MR fluids can be captured by using the generalized Kelvin–Voigt model that is constituted by a series association of a Maxwell liquid and a certain number of Kelvin–Voigt solids. According to this model, the creep compliance function can be written as (Tadros 1987) follows:

$$J(t) = \frac{\gamma}{\tau_0} = J_0 + \sum_{i=1}^{N} J_i \left(1 - e^{-t/t_i}\right) + \frac{t}{\eta_0} \tag{4}$$

and the recoil can be written as follows:

$$R(t) = \frac{\gamma_r}{\tau_0} = \frac{T}{\eta_{0r}} + \sum_{i=1}^{N} J_{ir} \left(e^{T/t_{ir}} - 1\right) e^{-t/t_{ir}} \tag{5}$$

Here, it is assumed that the stress is applied for $t < T$ and removed at $t = T$. Also, $t_i = \eta_i J_i$ represents the retardation time of the Kelvin–Voigt solid. For the experiments reported in this study, curves are well fitted, taking just one Kelvin–Voigt solid ($N = 1$). This description is particularly useful because all the data in the small strain region should collapse to the shear compliance function if the MR fluid is responding in the linear viscoelastic regime. The first term in the RHS of Eq. 4 represents the elastic + plastic property of the MR fluid, the second term is associated to the delayed elastic strain, and finally, the third term is associated to the irreversible viscous flow. If the stress is applied for a long time, the sample may deform permanently, and the viscosity at the corresponding shear rate is given by the inverse of the slope of the compliance curves in this steady flow region. In the case of linear viscoelastic materials, J_0 must be elastically recovered upon cessation of the stress. However, in magnetized MR fluids, J_0 generally comprises two components, an elastic one and a plastic one (see below).

In Table 1, we show best-fitting parameters to Eqs. 4 and 5 for a wide range of magnetic fields investigated. Data in Table 1 reveal that the instantaneous compliance slightly increases when the stress value for all magnetic fields investigated increases. Strictly speaking, this point suggests that stresses applied are already out of the viscoelastic linear region. For all magnetic fields investigated, we could ideally identify three regions. (1) For low stresses, the compliance function has three contributions: instantaneous, retarded, and viscous flow. (2) Upon increasing the stress value, the retarded elastic and viscous components decrease, and at some critical stress, the MR fluid is instantaneously strained without the observation of retarded elastic and viscous components. At this stage, η_0 becomes infinite, and J_1 exhibits a very low negligible value (i.e., viscoplastic solid behavior). Similar findings were obtained by Otsubo and Edamura (1994). (3) For a larger stress value, $J_0 = 0$ and the MR fluid flows as a plastic fluid exhibiting a very low viscosity η_0. The stress value corresponding to this transition has been associated in the past with the viscosity bifurcation phenomena observed by Coussot and coworkers (2002) in highly thixotropic yield stress materials, and as a consequence, this stress value may be considered the frontier between the pre- and postyield regimes. Even though non-negligible values are obtained from data fitting for J_1 and t_1, the result of the fit is not sensitive to important changes in J_1 and t_1.

Table 1 Values of best-fitting parameters at each magnetic field strength according to Eqs. 4 and 5

Stress (Pa)	Creep test				Recovery test		
	J_0 (1/Pa)	η_0(Pa·s)	J_1(1/Pa)	t_1(s)	η_{0r}(Pa·s)	J_{1r}(1/Pa)	t_{1r}(s)
52 kA/m							
5	0.0047	250,000	0.0012	16	64,000	0.001	14
10	0.0065	410,000	0.00096	4.6	57,000	0.0021	0.46
15	0.010	1,100,000	0.00156	2.6	32,000	0	–
30[a]	0.038	∞	0	–	8,400	0	–
60[a]	0.11	∞	0	–	2,700	0	–
100	*0*	*56*	*2.7*	*40*	*39*	*0*	–
300	*0*	*5.2*	*20*	*78*	*3.8*	*0*	–
500	*0*	*0.17*	*200*	*80*	*0.15*	*0*	–
86 kA/m							
20	0.0043	1,300,000	0.00039	1.8	78,000	0.00052	0.46
60	0.012	∞	0.0016	1.9	25,000	0.00088	0.45
100	0.0073	∞	0	–	42,000	0.00061	0.46
150	0.018	∞	0	–	18,000	0.000092	0.45
300[a]	*0*	*300*	*3.1*	*47*	*72*	*0*	–
500	*0*	*18*	*4.7*	*50*	*14*	*0*	–
800	*0*	*5.3*	*3.4*	*65*	*5.0*	*0*	–
1, 000	*0*	*3.4*	*3.0*	*68*	*3.3*	*0*	–
173 kA/m							
50	0.00038	1,900,000	0.000020	8.1	990,000	0.000089	87
150	0.0015	∞	0.000074	0.9	250,000	0.000035	1
250	0.0020	∞	0.00013	1.14	180,000	0.0001	0.5
400	0.0062	∞	0.00077	1.85	45,000	0.0001	0.5
600[a]	0.042	∞	0.00057	11.28	7,200	0.00002	0.5
1, 000[a]	*0*	∞	*1.35*	*14.9*	*210*	*0*	–
1, 500	*0*	*18*	*2.05*	*41*	*16*	*0*	–
1, 800	*0*	*8.5*	*0*	–	*8*	*0*	–
259 kA/m							
100	0.00040	3.800,000	0.000011	1.3	1,100,000	0.000047	41
500	0.0049	∞	0.00046	1.5	60,000	0	–
1,000[a]	0.097	∞	0.049	5.7	1,100	0	–
1, 400[a]	*0*	∞	*0.69*	*12*	*320*	*0*	–
1, 800	*0*	*60*	*1*	*30*	*51*	*0*	–
1, 900	*0*	*39*	*0.068*	*13*	*39*	*0*	–
2, 200	*0*	*16*	*0*	–	*15*	*0*	–
2, 600	*0*	*7.4*	*0*	–	*6.9*	*0*	–

Italicized values correspond to the fluidized (plastic fluid) region

[a]Measurements where a stepwise increase in strain is observed

Regarding the recovery behavior, we should say that the response is very slightly retarded as inferred from the low values of J_{1r} in Table 1. As a consequence, the recovery is nearly instantaneous and essentially given by the first term in Eq. 5 (T/η_{0r}). As observed in Table 1, η_{0r} decreases when the stress value independent of the magnetic field strength increases. Importantly, a sudden drop in η_{0r} is observed at a shear stress close enough to the yielding point and associated to the maximum in Fig. 5a that manifests a purely viscous fluid flow.

It is also important to remark that stress values that are marked with a) in Table 1 correspond to those cases where a stepwise increase in the strain was monitored. Similar findings were reported in the past by Otsubo and Edamura

(1994) and Li et al. (2002). This stepwise increase in the strain close to the critical yield stress value has been claimed to be due to field-induced chain rupture and reformation under shear.

Comparison between steady shear flow curves and creep tests: viscosity bifurcation

A further insight on the creep behavior can be obtained when plotting the instantaneous viscosity, defined as the ratio between the stress and the shear rate, as a function of time (see Fig. 6). This kind of representation has been traditionally employed (Coussot et al. 2002; Moller et al. 2006, 2009a) to investigate the yielding behavior of pastes and demonstrated the appearance of the previously commented viscosity bifurcation at the yield stress in the case of highly thixotropic yield stress fluids (Coussot et al. 2002) and a change in the viscosity versus time slope in the case of non-thixotropic yield stress fluids. Below the yield stress, the viscosity of non-thixotropic yield stress fluids keeps slowly increasing in time as $\eta \propto t^{0.6}$ for times even longer than 10^4 s (Moller et al. 2009b). In contrast, for non-thixotropic yield stress fluids above the yield stress, the viscosity quickly reaches a steady (constant) value. The structural models discussed above (Quemada 2008; Coussot et al. 2002) provide further insights to interpret these phenomena, at least qualitatively. Additional discussions are given below in relation to Fig. 10.

Results shown in Fig. 6 demonstrate a slow flow that appears to occur at long times in the preyield regime as indicated by the fact that the curves for the lowest stresses do not become perfectly horizontal lines but continue to rise ($\eta \propto t$). Even though these measurements are well inside the rheometer resolution, the very low values of the shear rate involved make this part of the measurement susceptible to possible sample slippage and instrument noise effects.

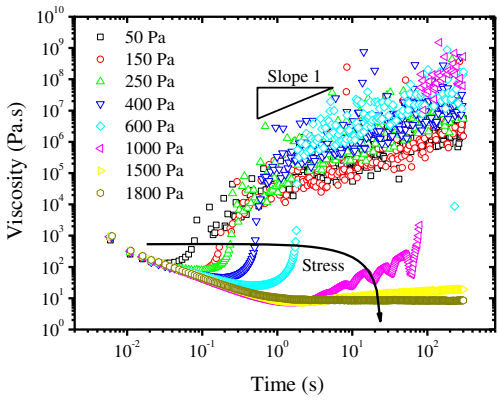

Fig. 6 Instantaneous viscosity as a function of time for constant stress values for 5 vol% MR fluid. The magnetic field strength is 173 kA/m

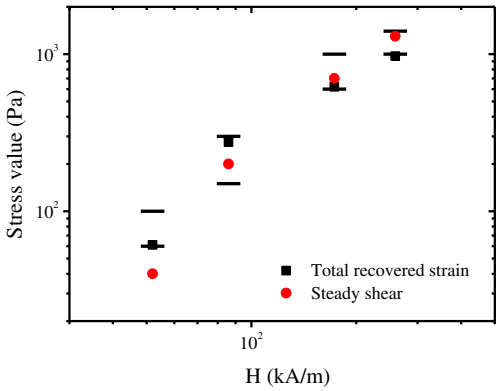

Fig. 7 Yield stress as a function of the external magnetic field in 5 vol% MR fluids. *Horizontal lines* correspond to the *upper* and *lower* bounds as obtained from viscosity bifurcation representations (Fig. 6). *Squares* correspond to those stresses where the ratio of recovered strains becomes zero (Fig. 5b). *Circles* represent the yield stresses obtained from the extrapolation in steady shear flow curves (Fig. 3b)

Similar findings were reported for commercial MR fluids by See et al. (2004).

At this stage, it would be interesting to compare the yield stress obtained from steady shear flow curves and creep tests. In Fig. 7, we show such a comparison. As observed, steady shear and unsteady shear creep experiments provide yield stress data that are in reasonably good agreement. Actually, our results reveal that the yield value inferred from the maximum in the total recovered strain is in reasonably good agreement with the static yield stress obtained from steady shear flow curves. Contrary to our observations, Otsubo and Edamura (1994) reported a yield stress value from creep tests that were about 70 % of the plateau stress in steady shear flow curves.

Comparison with model yield stress fluids

As demonstrated above, MR fluids are yield stress fluids in the sense that they hardly flow if the imposed stress is below a certain (field-dependent) value, but they flow at high shear rates when the stress exceeds the so-called yield stress τ_Y.

It has been recently reported that yield stress fluids can be categorized in two groups: thixotropic and non-thixotropic (simple) yield stress fluids. Even though, in the past, the phenomena of yield stress and thixotropy have been considered separate fields of research, currently, they are demonstrated to be intimately linked (Moller et al. 2006; Coussot et al. 2006). On the one hand, an ideal simple (non-thixotropic) yield stress fluid is one for which the shear stress depends only on the shear rate. In this case, viscosity diverges continuously when the yield stress is approached from above. Typical examples involve foams, emulsions, and microgels. On the other hand, in (highly) thixotropic

yield stress fluids, the stress depends both on the (instantaneous) shear rate and the shear history of the sample. By far, the vast majority of yield stress materials are highly thixotropic. In thixotropic materials, the stress reversibly decreases with time at high shear and increases with time under rest or low shear rates. As a consequence, a typical test frequently used to ascertain whether a material is thixotropic or not is increasing the shear stress/rate and then decreasing it while continuously measuring the resulting shear rate/stress. If the stress is not a function of the shear rate only but also depends on the history of the sample, the two curves should not collapse, and the material is said to be (highly) thixotropic. Typical examples of (highly) thixotropic materials are clay suspensions and colloidal gels.

According to the discussion above, a carefully controlled measurement protocol must be followed to get reliable and reproducible results. As a consequence, prior to a test, yield stress fluids must be brought to the same initial state by a controlled history of shear and rest in what rheologists call a "preshear" stage.

Two model yield stress materials are employed in this work to compare their yielding behavior with that of conventional MR fluids. On the one hand, polyacrylic acid-based microgel suspensions are employed as a representative example of simple yield stress fluids because they are very slightly thixotropic. On the other hand, bentonite clay suspensions are used as model (highly) thixotropic fluids. The particular formulations of these colloidal systems were chosen ad hoc for them to have a similar yield stress value under the same experimental conditions.

1. Microgel suspensions employed in this work are highly cross-linked anionic polyacrylic acid (PA) that swells upon neutralization to form electrically charged particles of approximately a few microns diameter (de Vicente et al. 2006; Gutowski et al. 2012). Concentrations of approximately 0.1 wt% are reported in the literature to be sufficient for the particles to jam together to form a yield stress fluid. The weight concentration employed was 0.5 wt%. The pH was adjusted by adding sodium hydroxide.
2. Weakly flocculated clay suspensions were prepared by dispersion of bentonite clay (BC) in water. The weight concentration employed was 10 vol%. The reason for this concentration value is that the yielding behavior of these particular systems has been extensively reported in the literature. Actually, data for increasing and decreasing stress ramps have been reported by Moller et al. (2009a).
3. Unless appropriately stabilized, MR fluids are well-known to exhibit important sedimentation problems because of the large density mismatch between the constituent iron particles and dispersing medium. To ensure that MR fluids remain stable at least during the rheology tests and, in particular, during the quiescent period at the preshear stage, we did increase the viscosity of the dispersing medium. Hence, silicone oils employed in the formulation of MR fluids employed in this section had a viscosity of 487 mPa·s. By simply increasing the viscosity of the dispersing medium, iron microparticles are expected to remain in suspension in longer periods of time, and importantly, the yield stress is not expected to be much influenced at a given magnetic field strength. The particle concentration remained fixed at 5 vol%. When dealing with MR fluids, magnetic fields applied were 53 kA/m in order for the yield stress to be of a similar order of magnitude than the yield stress of PA and BC suspensions.

Steady shear flow

Getting reproducible results is notoriously difficult, especially with highly thixotropic yield stress fluids, because of their shear history. Consequently, a strict experimental protocol was followed to ensure reproducibility and comparability. Steady shear flow curves were ascertained following the protocol described in Fig. 8. For initial conditioning, the samples were subjected to steady shearing at 100 s^{-1} for 200 s and left (magnetized if needed) in a quiescent state for 200 s. Subsequently, the test was started. To confirm that 200 s was sufficiently long for the microscopic structures to form, a series of tests were carried out using different intervals of time in the quiescent state. It is worth to stress here that a preconditioning is absolutely necessary to get reliable and reproducible results. Steady shear flow curves were obtained here using stress- and strain-controlled modes in order to more clearly differentiate between the so-called static and dynamic yield stresses.

Results obtained using the protocol described in the above paragraph are shown in Fig. 9 for the three systems investigated. In the case of PA, we clearly observe that both up and down stress curves do essentially overlap, suggesting that under the experimental conditions, microgel suspensions behave as non-thixotropic yield stress fluids. Note that in this case, the stress increases/decreases 1 Pa every 3 s, and this is a long time enough for the microgel suspension to reach a pseudo-steady state. As we will see later, the steady state is reached in only 1 or 2 s (see Fig. 10a). Importantly, the non-thixotropic character is manifested by using both stress- and strain-controlled tests. Actually, the steady shear rheology of PA microgels is fit extremely well by the Herschel–Bulkley model (Moller et al. 2006; 2009a, b; Gutowski et al. 2012). As shown in Fig. 9a, the yield stress of PA suspensions is around 20 Pa. As expected, this is a much smaller value than the Bingham one predicted from

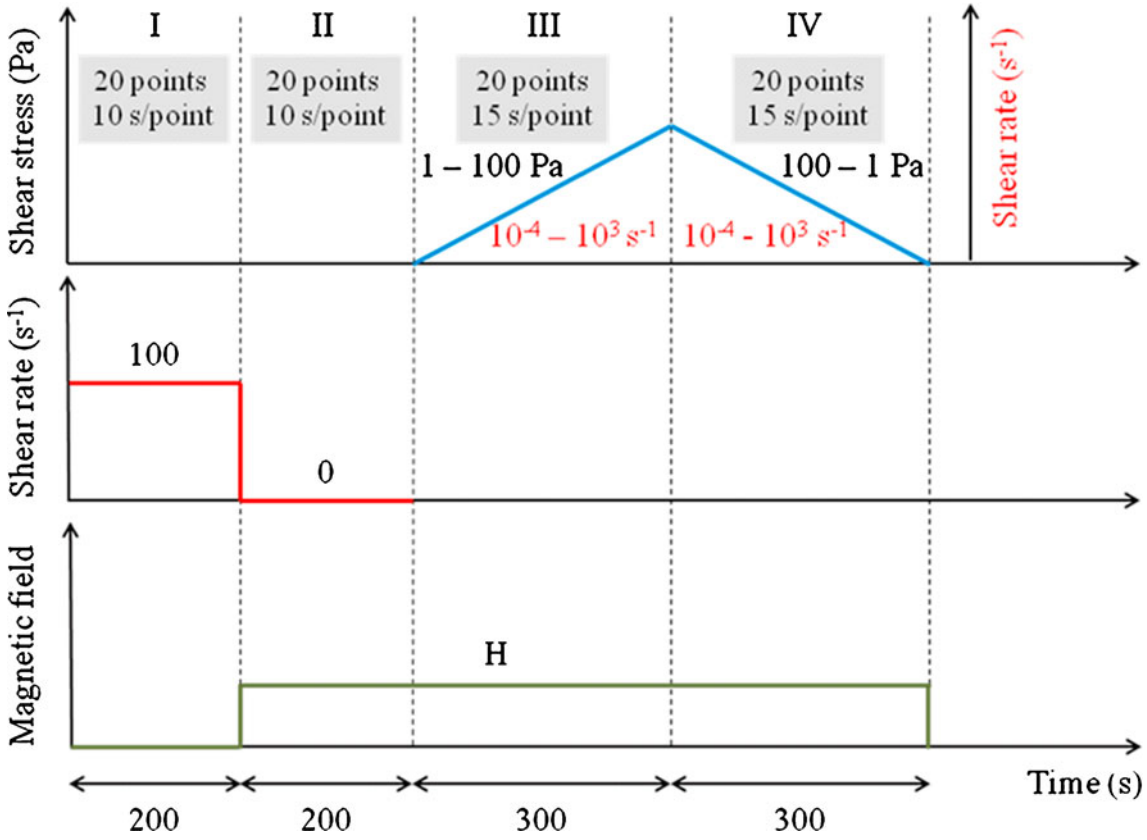

Fig. 8 Schematic of the protocol used for the steady shear flow curve investigations. Not to scale

lineal regression, at large deformation, to stress/shear rate data in Fig. 9b.

Similar to PA suspensions, data for increasing and decreasing shear stresses in MR fluids coincide (cf. Fig. 9a). These results are further checked through strain-controlled tests up to shear rates of 400 s^{-1} (cf. "MR fluid (MRF) short" data in Fig. 9b). As a consequence, a priori MR fluids formulated here in a high viscosity dispersing medium can be considered as non-thixotropic yield stress materials. In our case, the static yield stress in MR fluids is around 70 Pa (cf. Fig. 9a), while the dynamic/Bingham yield stress value is found to be very similar to that of PA suspensions (approx. 500 Pa, cf. Fig. 9b). For completeness, in Fig. 9b, we include up-and-down shear rate ramps covering a larger shear rate range (up to 1,000 s^{-1}) where the isotropic–nematic transition for MR fluids is observed (for further details, see Volkova et al. 1999). For the purpose of the present study, we are only interested in the early stages of the yielding process, and consequently, we will not achieve large enough shear stresses (shear rates) for the development of the isotropic–nematic transition.

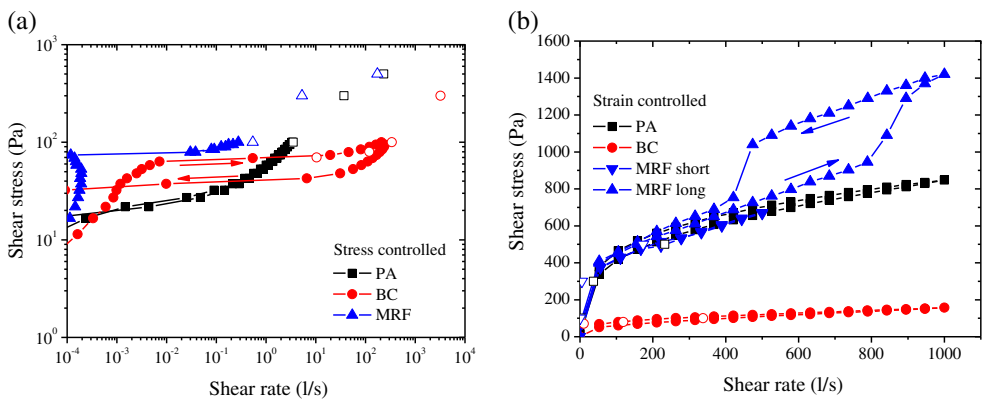

Fig. 9 Up-and-down stress curves of (**a**) stress controlled, (**b**) strain controlled. *Open symbols* correspond to steady shear viscosity values obtained from Fig. 10

Finally, BC suspensions do clearly exhibit a thixotropic loop. This was expected as the weakly flocculated clay suspension liquefies at high stresses, and then, the branch obtained upon decreasing the stress is significantly below the one obtained while increasing the stress. This is clearly seen in the kind of representation employed in Fig. 9a. Note that contrary to PA suspensions, in this case, 3 s is not enough for the BC suspensions to reach a steady state (see Fig. 10b in the following sections). The yield stress for BC suspensions as obtained from the up stress curve is very similar to that obtained for MR fluids (approx. 60 Pa).

It is worth to stress here that employing a lower viscosity silicone oil in the formulation of the MR fluid would result in a false thixotropic behavior due to the sedimentation of field-induced structures in the down curve. As demonstrated in Fig. 9a, the use of a larger viscosity dispersing medium prevents such sedimentation. It is also important to report that, a priori, the yielding behavior of MR fluids should not depend on the viscosity of the dispersing liquid as soon as the particle concentration and magnetic field strength remain constant. As will be shown later, the yield stress value for MR fluids formulated with different oil viscosities is essentially the same in spite of using different preshearing protocols.

Creep–recovery tests

Creep tests were also carried out in model yield stress fluids using the same preconditioning protocol (stages I and II in Fig. 8) as described above and with the same acquisition times as reported in Fig. 2. Additionally, we did also check that running concatenated creep/recovery tests after step V in Fig. 2 gave the same results for PA and MR fluids which were found to be non-thixotropic materials. On the other hand, as expected because of their thixotropic behavior, in the case of BC suspensions, concatenated tests gave different results because of the aging of the suspension.

Results obtained for PA-based (simple) yield stress fluids are shown in Fig. 10a. As observed, a few seconds after the shear stress is applied, the viscosity seems to reach a steady value for the larger stresses applied. However, for low stresses, curves obtained seem to deviate from this observation. The observed transitionary stress is interpreted in the literature as the yield stress. In the classical rheology literature, this kind of simple yield stress fluid has been taken as an example to show that yield stress materials do not really exist but, instead, behave as very high viscosity materials at low shear (Barnes 1999). However, more recently, this observation has been questioned (Moller et al. 2006) by running creep measurements for times as long as 10^4 s in nonslip samples. In the time interval investigated here, the viscosity value seems to reach a clear steady plateau value for large stresses. On the other hand, similar to Moller et al. (2006), a slow flow appears here to occur at long times in the low stress regime that is well inside the rheometer's resolution. For these low stresses, the viscosity has been reported to increase with time following a power law with exponents that range from 0.6 for 2 % Carbopol suspensions to 1.0 for hair gels (Moller et al. 2009a). This increase with time is generally found to be independent of the stress value and is associated to *overaging* of the sample.

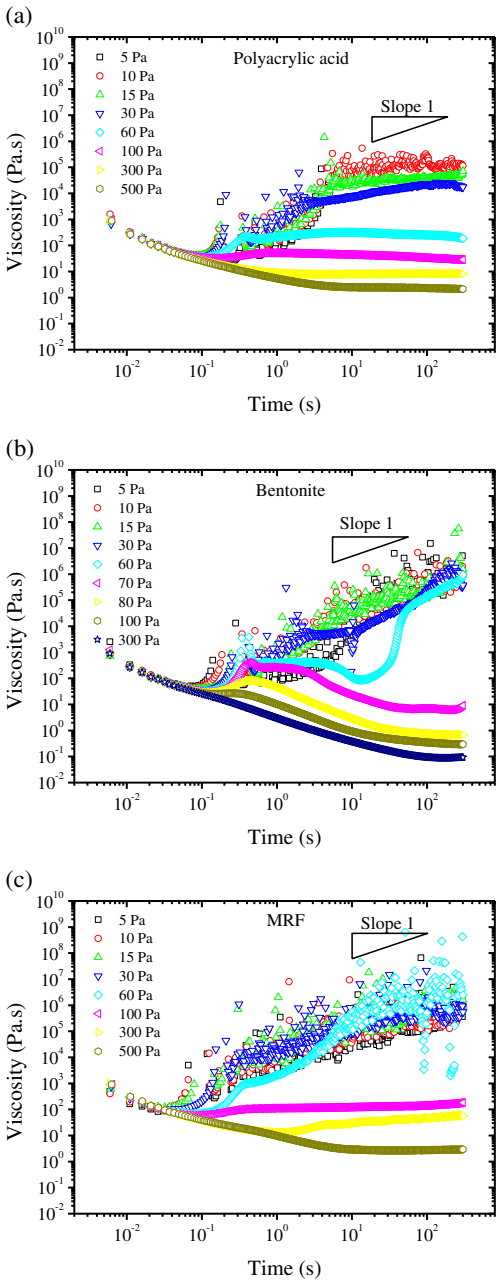

Fig. 10 Instantaneous viscosity as a function of time for different imposed stresses. **a** Microgel suspension, **b** clay suspension, **c** MR fluid

At this point, one should note that, strictly speaking, microgels are not free of thixotropy but present characteristic structuring times that are much shorter than those of bentonite clay suspensions, which is included here as a model thixotropic fluid (see Fig. 10b and discussions below). The subtle thixotropic behavior of microgels does not manifest in the timescales of the experiment associated to Fig. 9 but becomes evident in Fig. 10a, where one observes that the system takes times around 1 s to reach the equilibrium viscosity, for the highest stresses applied.

Results for BC suspensions are included in Fig. 10b. This kind of representation highlights the viscosity bifurcation and avalanche phenomena characteristic of (highly) thixotropic yield stress fluids such as BC suspensions. Contrary to what occurs in the case of microgel suspensions, now the viscosity very clearly increases with time at low stresses, and a non-monotonic behavior is observed for intermediate stress levels. It has been reported in the past that buildup (aging) of the structure wins over the destruction (rejuvenation) of it when thixotropic yield stress fluids are subjected to low stress values (below a critical yield stress). As a consequence, the shear rate enormously decreases, and hence, the viscosity increases quadratically in time "until the flow is halted altogether" (Moller et al. 2006; Quemada 2008). On the other hand, for slightly larger stress values than the yield stress, the viscosity decreases by many orders of magnitude in an avalanche mode describing a discontinuous transition (viscosity bifurcation). In terms of the structural model (Quemada 2008), the viscosity plateaux for $\tau > \tau_Y$ involve a dynamic equilibrium between structuring and destructuring processes, i.e., $dS/dt = 0$. The system may approach the equilibrium by either breaking down ($dS/dt < 0$) or building up ($dS/dt > 0$) the structure. At intermediate shear stresses, the plateaux appear to be instable, which may be due to the high sensitivity to the imposed shear stress values in the close vicinity of the bifurcation (Fig. 1b). An outstanding difference when comparing Fig. 10a, b comes from the appearance of a shoulder in the case of BC suspensions. This can be easily explained because the suspension ages during the rest stage as demonstrated in Fig. 9a. Hence, for large enough stresses, $\tau > \tau_K$, viscosity must decrease to reach a steady value (see Fig. 1b).

Experimental data corresponding to the MR fluids are included in Fig. 10c. Results obtained qualitatively behave in an intermediate way between PA and BC suspensions and closely resemble measurements carried out in sections above where the effect of magnetic field strength was explored. A quick look to the figures reveals that the low stress behavior of MR fluids is very similar to the one of BC suspensions. On the other hand, the high shear stress regime looks more alike to the PA suspensions. In other words, Fig. 10c shows that the viscosity of MRF quickly reaches a steady value for the larger stresses imposed, which

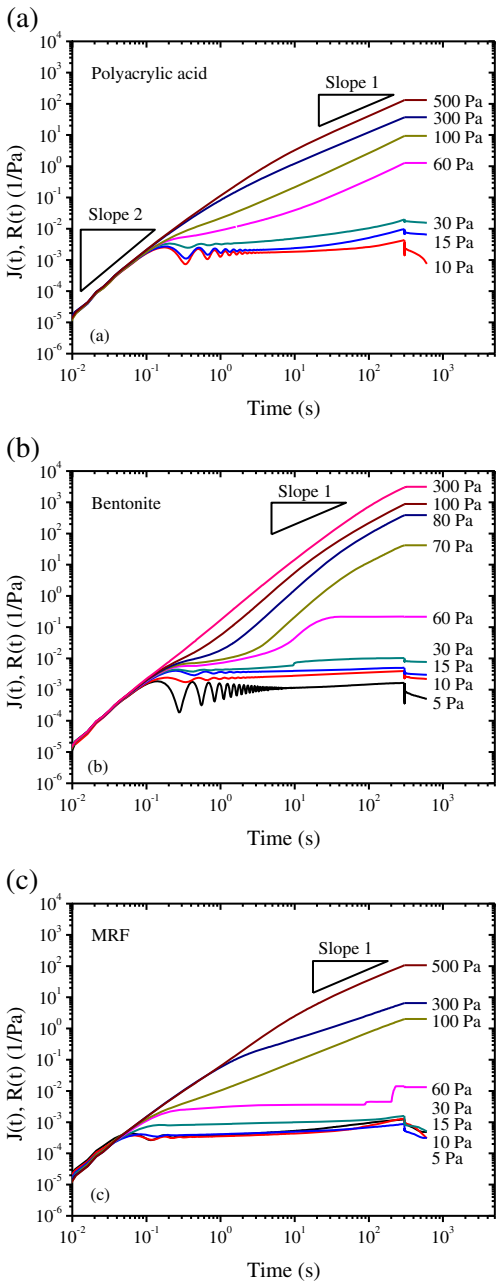

Fig. 11 Time dependence of the shear creep compliance $J(t)$ and recoil $R(t)$ functions for the three systems investigated: **a** microgel suspension, **b** bentonite suspension, **c** MR fluid. The initial noise in the compliance at low stresses is presumably caused by inertio-elastic effects

is a characteristic of systems virtually free of thixotropy, as discussed above for PA suspensions. However, at the lowest stresses, the viscosity continuously increases during the times observed, and the fluid seems to age similar to BC suspensions.

Again, more valuable information can be obtained in terms of the compliance and recoil functions corresponding to the creep and recovery stages. Results obtained for the three

systems investigated are included in Fig. 11. This kind of representations clearly manifests the differences described above. The quadratic dependence of the strain with the time and the oscillations at short times may correspond to the response of the (viscoelastic) material when it is suddenly submitted to a shear stress, while there is a significant inertia of the system. In fact, a similar ringing has been described in the literature in the past in other different materials (e.g., Coussot et al. 2006).

To get further information, compliance and recoil curves shown in Fig. 11 were fitted to Eqs. 4 and 5. The parameters obtained from the fits are included in Table 2. As observed in Table 2, the instantaneous compliance remains at a very low constant value for the lowest stresses investigated. This suggests that in this case, the systems essentially behave in the viscoelastic linear region. In Fig. 12a, we show that in spite of this, the behavior of the three systems under the viscoelastic linear region (for a given stress value applied of 15 Pa) is pretty different. On the one hand, the smallest η_0 is obtained for PA suspensions. On the other hand, the largest J_0 is obtained in the case of MR fluids.

The fact that the suspensions behave in the viscoelastic linear region is further confirmed in Fig. 12b where we find a quantitative good agreement between the low strain storage modulus (solid line in Fig. 12b) and the instantaneous strain/applied stress relation from creep tests (symbols in Fig. 12b) up to stress values of approximately 30 Pa. Again, this finding is also in good agreement with the fact that the instantaneous strain coincides with the instantaneously recovered strain at low stress levels (see Fig. 12c). Finally,

Table 2 Same as Table 1 for microgel suspensions (PA), clay suspensions (BC), and MR fluids (MRF)

Stress (Pa)	Creep test				Recovery test		
	J_0(1/Pa)	η_0(Pa·s)	J_1(1/Pa)	t_1(s)	η_{0r}(Pa·s)	J_{1r}(1/Pa)	t_{1r}(s)
PA							
10	0.0017	120,000	0.00014	7.3	270,000	0.0016	83
15	0.0020	49,000	0.0018	110	44,000	0.0012	24
30	0.0034	23,000	0.00247	32	19,000	0.0024	96
60	*0*	*250*	*0*	–	*240*	*0.0038*	*200*
100	*0*	*35*	*0*	–	*32*	*0*	–
300	*0*	*8.1*	*0*	–	*8.2*	*0*	–
500	*0*	*2.4*	*0*	–	*2.3*	*0*	–
BC							
5	0.0011	200,000,000	0.00057	86	520,000	0.00039	43
10	0.0025	570,000	0.00098	31	520,000	0.0056	590
15	0.0036	400,000	0.00079	21	93,000	0.0011	0.45
30	0.0056	3,900,000	0.0047	30	38,000	0.0015	0.45
60[a]	–	–	–	–	1,400	0.00045	0.46
70	*0*	*7.5*	*0*	–	*7.2*	*0*	–
80	*0*	*0.87*	*0*	–	*0.78*	*0*	–
100	*0*	*0.39*	*0*	–	*0.34*	*0*	–
300	*0*	*0.11*	*0*	–	*0.099*	*0*	–
MRF							
5	0.00046	4,900,000	0.00072	96	610,000	0.00052	67
10	0.00037	560,000,000	0.0018	390	3,900,000	0.00128	230
15	0.00044	1,000,000	0.00015	41	890,000	0.00025	56
30	0.00089	510,000	0.00011	8.9	390,000	0.0005	0.46
60[a]	–	–	–	–	23,000	0.00056	0.46
100	*0*	*∞*	*5.7*	*710*	*150*	*0*	–
300	*0*	*51*	*0.75*	*29*	*46*	*0*	–
500	*0*	*2.8*	*0*	–	*2.8*	*0*	–

MR fluids investigated in this table are different to those reported in Table 1

Italicized values correspond to the fluidized (plastic fluid) region

[a]Measurements where a stepwise increase in strain is observed

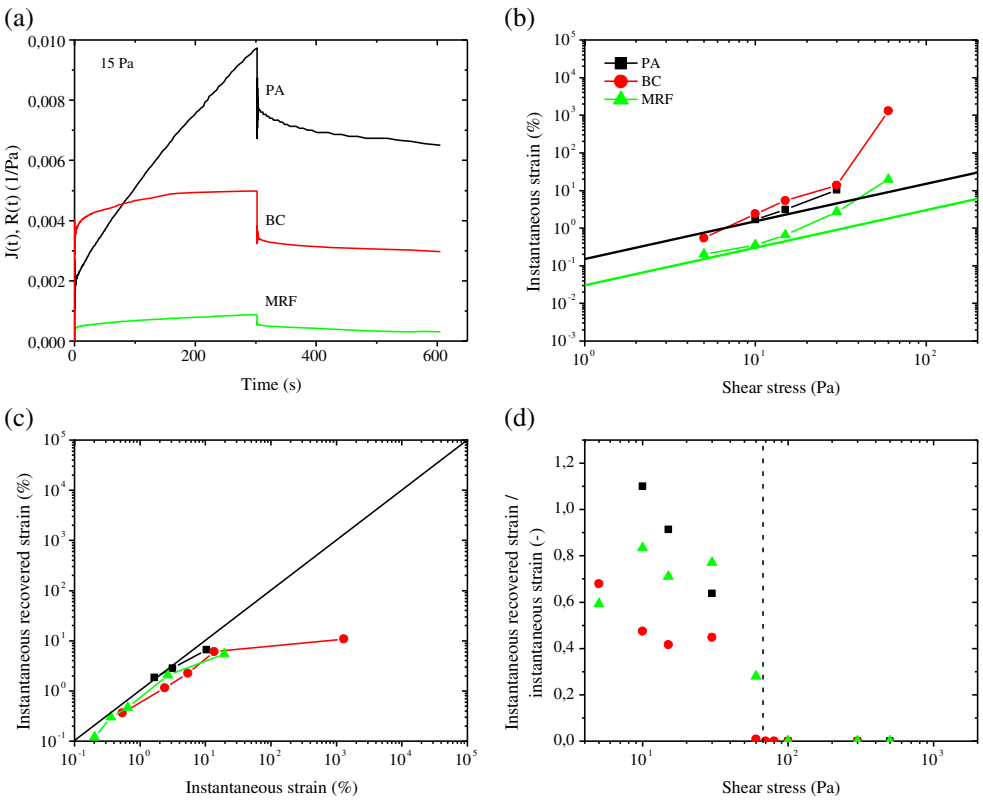

Fig. 12 Characterization of the preyield regime and onset of nonlinearity in PA, BC, and MRF systems: **a** compliance and recoil functions in the preyield regime, **b** instantaneous strain as a function of the applied shear stress. *Solid lines* are taken from the low-strain storage modulus. **c** Instantaneously recovered strain as a function of the instantaneous strain at the onset of creep, **d** ratio between the instantaneously recovered strain and the instantaneous strain as a function of the shear stress

deviation from linearity is also achieved at a very similar stress (≈60 Pa) and strain (≈10 %) levels (cf. Fig. 12d).

Throughout this work, the yielding behavior of conventional MRF has been investigated by using steady shear and creep–recovery tests, in order to elucidate if these fluids exhibit time-dependent phenomena like aging and thixotropy. At very low stress levels, MR fluids behave in the linear viscoelastic regime and evolve towards nonlinear viscoelastic, viscoplastic, and plastic responses when the stress value is increased. In steady shear flow, a plastic fluid behavior is found when the imposed stress is larger than the so-called yield stress. Finally, creep–recovery test showed that MR fluids might involve the aging phenomena akin to thixotropic fluids at low shear stresses, while an almost non-thixotropic behavior is exhibited at higher stresses.

Conclusions

In the literature, tests involving MR fluids typically focus on the response at shear rates over 1 s^{-1} (See et al. 2004). However, MR fluids are demonstrated to deviate from plastic fluid models (Bingham, Herschel–Bulkley, etc.) because the latter assume that the MR fluid operating in the preyield regime does not deform at all if the applied stress is below a critical yield stress value (Berli and de Vicente 2012). In this sense, unsteady creep tests are found to be interesting because they do actually provide further insight into the yielding mechanism under the presence of magnetic fields. Indeed, experiments reported here demonstrate that MR fluids do *creep* even under the presence of stresses below the "yield" stress.

In the case of dilute MR fluids subjected at very small stress levels, the instantaneously recovered strain is anticipated to be very similar to the instantaneous strain as expected from the linear viscoelasticity theory. This is so because field-induced structures slightly deform under the applied stress and later recover. In this situation, particle aggregates fully connect the plates, generating an elastic response that is later released when the stress is removed. The stresses investigated in the first part of this work are generally too large to observe this region. See et al. (2004) reported that the linear response occurs for strains of the order of 0.1 % or smaller.

For larger stresses, the energy used to stretch the field-induced structures is not completely stored, and partial dissipation occurs. This finding has been previously described in the literature by Otsubo and Edamura (1994) and Li et al. (2002) and interpreted by the deformation of clusters of particles arranged in a BCT lattice. In general, this is possibly due to the existence of structures that are attached at only one plate or are completely free (i.e., unattached). The deformations of free and unattached chains are expected to generate a plastic response.

For stresses very close to the yield stress, the stored energy is consumed, and the field-induced structure changes to another metastable configuration. The suspension is almost instantaneously strained without viscous flow, and in this case, the MR fluid will not exhibit an elastic recovery. The MR fluid behaves as a plastic fluid and exhibits a stepwise increase in the strain during the creep period.

For very large stresses, the field-induced structure is destroyed, and the system flows with a low viscosity level. Obviously, the system does not recover the strain upon the cessation of the stress.

Experiments reported here basically concern systematic creep tests with different stress values at a constant time of rest (waiting time). With this, it is possible to study the solid–liquid transition. However, MR fluids and soft glassy systems, in general, exhibit two directly related characteristics, namely, jamming and aging, that are mechanically manifested by the yielding and thixotropic behavior. In our opinion, to better understand the aging of these systems, future work should involve the study of the effect of the time of rest.

Acknowledgments This work was supported by MICINN MAT 2010-15101 project (Spain), by the European Regional Development Fund (ERDF), and by Junta de Andalucía P10–RNM–6630 and P11–FQM–7074 projects (Spain). CB also acknowledges the financial support from the Universidad Nacional del Litoral and the Consejo Nacional de Investigaciones Científicas y Técnicas, Argentina.

References

Barnes HA (1999) The yield stress—a review or everything flows. J Non-Newton Fluid Mech 81:133–178

Barnes HA, Nguyen QD (2001) Rotating vane rheometry—a review. J Non-Newton Fluid Mech 98:1–14

Berli CLA, de Vicente J (2012) A structural model for magnetorheology. Appl Phys Lett 101:021903

Berli CLA, Quemada D (2000) Rheological modeling of microgel suspensions involving solid–liquid transition. Langmuir 16:7968–7974

Brady JF (1993) The rheological behavior of concentrated colloidal dispersions. J Chem Phys 99:567–581

Chotpattananont D, Sirivat A, Jamieson AM (2006) Creep and recovery behaviors of a polythiophene-based electrorheological fluid. Polymer 47:3568–3575

Christopoulou C, Petekidis G, Erwin B, Cloitre M, Vlassopoulos D (2009) Ageing and yield behavior in model soft colloidal glasses. Phil Trans R Soc A 367:5051–5071

Coussot P, Nguyen QD, Huynh HT, Bonn D (2002) Viscosity bifurcation in thixotropic, yielding fluids. J Rheol 46:573–589

Coussot P, Tabuteau H, Chateau X, Tocquer L, Ovarlez G (2006) Aging and solid or liquid behaviour in pastes. J Rheol 50:975–994

Craciun L, Carreau PJ, Heuzey M-C, van de Ven TGM, Moan M (2003) Rheological properties of concentrated latex suspensions of poly(styrene-butadiene). Rheol Acta 42:410–420

de Vicente J, González-Caballero F, Bossis G, Volkova O (2002) Normal force study in concentrated carbonyl iron magnetorheological suspensions. J Rheol 46(5):1295–1303

de Vicente J, Klingenberg DJ, Hidalgo-Álvarez R (2011) Magnetorheological fluids: a review. Soft Matter 7:3701–3710

de Vicente J, Stokes JR, Spikes HA (2006) Soft lubrication of model hydrocolloids. Food Hydrocolloids 20:483–491

Derec C, Ajdari A, Lequeux F (2001) Rheology and aging: a simple approach. Eur Phys J E 4:355–361

Derec C, Ducouret G, Ajdari A, Lequeux F (2003) Aging and nonlinear rheology in suspensions of polyethylene oxide–protected silica particles. Phys Rev E 67:061403

Gutowski IA, Lee D, de Bruyn JR, Frisken BJ (2012) Scaling and mesostructure of Carbopol dispersions. Rheol Acta 51:441–450

Heyes DM, Sigurgeirsson H (2004) The Newtonian viscosity of concentrated stabilized dispersions: comparisons with the hard sphere fluid. J Rheol 48:223–248

Laurati M, Egelhaaf SU, Petekidis G (2011) Nonlinear rheology of colloidal gels with intermediate volume fraction. J Rheol 55:673–706

Li WH, Du H, Chen G, Yeo SH (2002) Experimental investigation of creep and recovery behaviors of magnetorheological fluids. Mater Sci Eng A333:368–376

Moller PCF, Fall A, Bonn D (2009b) Origin of apparent viscosity in yield stress fluids below yielding. Eur Phys Lett 87:38004

Moller PCF, Fall A, Chikkadi V, Derks D, Bonn D (2009a) An attempt to categorize yield stress fluid behaviour. Phil Trans R Soc A 367:5139–5155

Moller PCF, Mewis J, Bonn D (2006) Yield stress and thixotropy: on the difficulty of measuring yield stress in practice. Soft Matter 2:274–283

Otsubo Y, Edamura K (1994) Creep behavior of electrorheological fluids. J Rheol 38:1721–1733

Petekidis G, Vlassopoulos D, Pusey PN (2003) Yielding and flow of colloidal glasses. Faraday Discuss 123:287–302

Petekidis G, Vlassopoulos D, Pusey PN (2004) Yielding and flow of sheared colloidal glasses. J Phys Condens Matter 16:3955–3963

Pham KN, Petekidis G, Vlassopoulos D, Egelhaaf SU, Poon WCK, Pusey PN (2008) Yielding behavior of repulsion- and attraction-dominated colloidal glasses. J Rheol 52(2):649–676

Quemada D (1977) Rheology of concentrated disperse systems and minimum energy dissipation principle I. Viscosity–concentration relationship. Rheol Acta 16(1):82–94

Quemada D (1998) Rheological modelling of complex fluids: I. The concept of effective volume fraction revisited. Eur Phys J Appl Phys 1:119–127

Quemada D (2008) Aging, rejuvenation, and thixotropy in complex fluids: time-dependence of the viscosity at rest and under constant shear rate or shear stress. Appl Rheol 18:53298

See H, Chen R, Keentok M (2004) The creep behaviour of field-responsive fluids. Colloid Polym Sci 282:423–428

Segovia-Gutiérrez JP, Berli CLA, de Vicente J (2012) Non-linear viscoelasticity and two-step yielding in magnetorheology: a colloidal gel approach to understand the effect of particle concentration. J Rheol 56(6):1429–1448

Segovia-Gutiérrez JP, de Vicente J, Hidalgo-Alvarez R, Puertas AM (2013) Brownian dynamic simulations in magnetorheology. Soft Matter. doi:10.1039/C3SM00137G

Tadros TF (1987) Solid/liquid dispersions. Academic, London, p 293

Trappe V, Prasad V, Cipelletti L, Segre PN, Weitz DA (2001) Jamming phase diagram for attractive particles. Nature 411:772–775

Volkova O, Cutillas S, Bossis G (1999) Shear banded flows and nematic-to-isotropic transition in ER and MR fluids. Phys Rev Lett 82:233–236